INL/CON-23-75540-Revision-0

Initial Demonstration of New Griffin Capability for Simulating the Running-In Phase of Pebble-Bed Reactors with Multiphysics

April 2024

Joshua Thomas Hanophy, Yaqi Wang, Javier Ortensi, Paolo Balestra

Changing the World's Energy Future

INL is a U.S. Department of Energy National Laboratory operated by Battelle Energy Alliance, LLC

INL/CON-23-75540-Revision-0

Initial Demonstration of New Griffin Capability for Simulating the Running-In Phase of Pebble-Bed Reactors with Multiphysics

Joshua Thomas Hanophy, Yaqi Wang, Javier Ortensi, Paolo Balestra

April 2024

Idaho National Laboratory
Idaho Falls, Idaho 83415

http://www.inl.gov

Prepared for the
U.S. Department of Energy
Under DOE Idaho Operations Office
Contract DE-AC07-05ID14517

Initial Demonstration of New Griffin Capability for Simulating the Running-In Phase of Pebble-Bed Reactors with Multiphysics

Joshua Hanophy [1,*], Javier Ortensi[1], Paolo Balestra[1], Yaqi Wang[1]

[1]Idaho National Laboratory, Idaho Falls, Idaho/USA

[leave space for DOI, which will be inserted by ANS]

ABSTRACT

Griffin, a MOOSE (Multiphysics Object-Oriented Simulation Environment) based application targeting transient modelling of advanced reactors, has been used recently to model pebble-bed reactors (PBRs). The modelling effort has focused thus far on modelling the equilibrium core. A new capability to simulate the running-in phase of PBR operation has been added to Griffin. This work demonstrates the new capability with a coupled multiphysics running-in simulation. In addition to including fuel, moderator, and reflector temperature feedback, we deploy a proportional pebble feed controller and include dynamic control rod positioning. In this work, Griffin computes power densities in the core at each timestep of the running-in simulation and passes these to Pronghorn which models fluid flow and heat transfer to calculate temperatures that are passed back to Griffin and accounted for with temperature dependent cross-sections. The running-in results presented in this work have not been optimized, they are meant to demonstrate some features of the new capability. Future work will include optimization of important running-in features such as pebble feed control and control rod positioning.

Keywords: running-in, burn-in, pebble bed reactor, griffin

1. INTRODUCTION

The MOOSE (Multiphysics Object-Oriented Simulation Environment) [1] based reactor modelling tool Griffin has been used recently for analyzing both high-temperature gas-cooled and fluoride-salt-cooled pebble bed reactors (PBRs) [2, 3, 4, 5, 6, 7]. This analysis work has focused on equilibrium core configurations. PBRs can be fueled continuously while they operate. Since a PBR can be fueled continuously, the average burnup of the core can be maintained at the same level throughout operation; the amount of fuel burned producing power is exactly made up in the fresh feed of fuel pebbles. This is referred to as an equilibrium core. When a PBR is first started, the fuel in the reactor is fresh. The reactor power is increased over time and the average burnup of the fuel increases. This period of initial operation is referred to as the running-in period. An overview of important considerations for a running-in simulation are provided in Ref. [8] where the running-in phase phase of operation was simulated for the High Temperature Gas-Cooled Reactor Pebble-bed Module in China using the Very Superior Old Programs (VSOP) software [9]. Some important differences between VSOP and Griffin are reviewed in Ref. [6]. Both VSOP and Griffin use deterministic methods for solving neutron transport, a good example of a running-in simulation performed with Monte Carlo methods can be found in Ref [10].

An initial running-in simulation capability for Griffin was introduced in Ref. [11]. That work introduced the algorithms and some methodology for the running in simulation, but the model investigated in that

*joshua.hanophy@inl.gov

work had no multiphysics and assumed constant temperatures. For this work, multiphysics is added to the simulation by coupling Griffin with Pronghorn, the MOOSE-based application for modeling intermediate fidelity thermal-hydraulics [12]. Griffin computes and sends the power density within the core to Pronghorn which models fluid flow and heat transfer computing temperatures that are sent back to Griffin and used for cross-section interpolation. Additionally, control rods are now modelled. The model used in this work is described in the next section.

1.1. Model Description

The model used in this work is based on the 200 MW_{th} generalized PBR first introduced in References [13], but has been simplified significantly. The dimensions and geometry are shown in Figure 1a. The model is used in RZ-geometry and is similar to that used in [11] except that a control rod channel has been added to the model used here. Control material extends from the top of the control rod channel down to some specified height and the region below this specified height is reflector material. The same discretization of burnup space (discussed in Section 2) shown in Table 1 of Ref. [11] is used in this work.

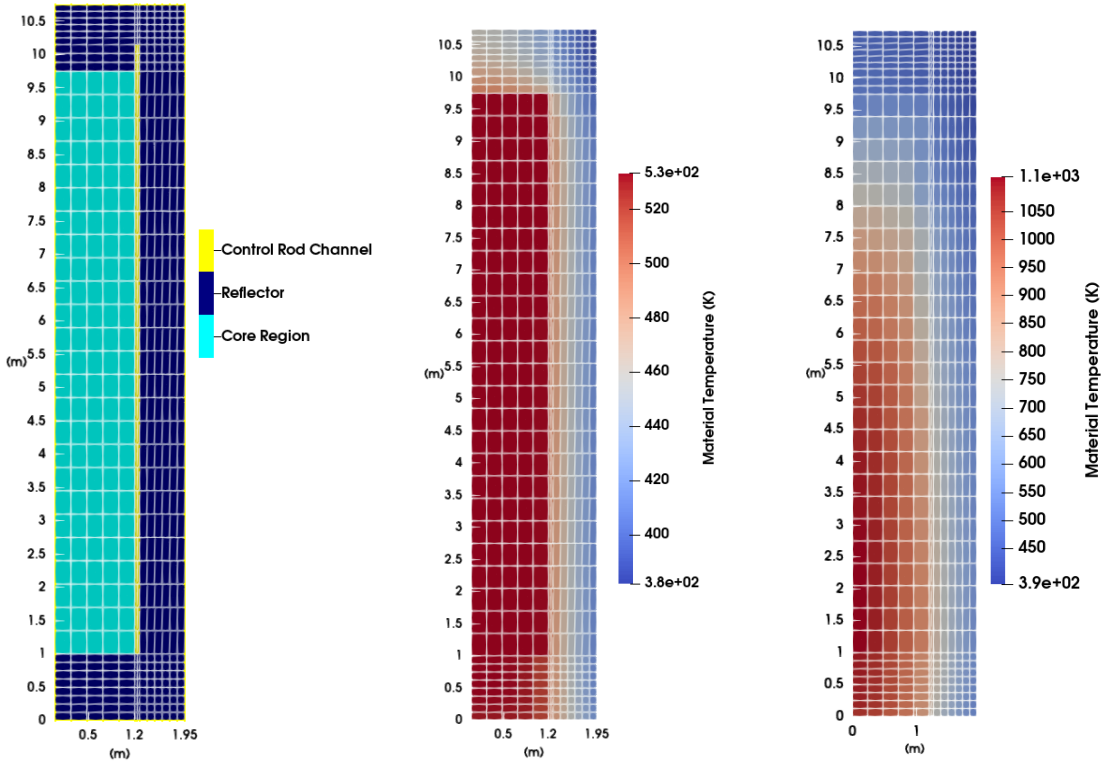

(a) **(b)** **(c)**

Figure 1. The material configuration of the model is shown in 1a. The initial material temperature for the running-in simulation is shown in 1b and the material temperature for the equilibrium core is shown in 1c.

1.1.1. Pronghorn model

The pronghorn model used in this work is similar to the one recently added [14] to the Virtual Test Bed (VTB) [3] (https://mooseframework.inl.gov/virtual_test_bed/htgr/generic-pbr-tutorial/index.html); however,

there are several important differences from the VTB model. First, the reflector geometry is different, the one used in this work is meant to more closely match an actual reactor geometry. Secondly, radiative and convective heat transfer boundary conditions have been added to the outside of the side reflector similar to those used in the higher fidelity model. The equilibrium core material temperatures for the simple model used in this work are shown in Figure 1c. The temperatures in this figure appear qualitatively similar to the temperature results from more sophisticated models, for example see Figure 3 in Ref. [4].

2. PBR MODELLING IN GRIFFIN

The methodology used in Griffin to model a PBR is discussed in detail in Ref. [6] and the basic points are reviewed in the section. Griffin uses a streamline approach to model the movement of pebbles and allows for the core region to have an unstructured mesh as well as features like a lower or upper cone. However; in the model used for this work, the streamlines correspond exactly to the mesh elements in the core region shown in Figure 1a and so streamlines are not discussed further. The pebbles flow only downward in space and so each column of cells in the core region represents a simple 1D flow problem. The burnup of pebbles is computed as part of the modelling approach used by Griffin. The burnup space of interest, from zero to some maximum value, is discretized into bins based on user input. An Eulerian approach is used and within each burnup bin – spatial mesh element cell, the conserved quantities computed are the volume fraction for each pebble type and the nuclide densities for each pebble type. The pebble volume fraction is written as $n_{c,k,l,m}$ for pebble type c, and the m_{th} mesh element in column k of elements, and burnup bin l. The nuclide densities are written as a vector for each nuclide tracked in the calculation as $\vec{N}_{c,k,l,m}$.

There is a flow of these quantities both in physical space, dictated by the flow velocity, and in burnup space, dictated by the power produced in the pebbles. The differential terms from these flows are discretized with simple upwinding resulting in the discrete equations shown in Equations 1 and 2 where a is a flow area, V a cell volume, $\Delta\tau$ is the width of a burnup bin, and $\bar{\rho}$ is the average power within a burnup bin. The average power is used because the conserved quantities are integrated over each burnup bin as $n_{k,l,m} = \int_{\tau_{l^-}}^{\tau_{l^+}} n(\tau)_{k,m}\, d\tau$, where τ_{l^+} and τ_{l^-} are the bounds of burnup bin l, so that the computed quantities are densities in physical space instead of in burnup and physical space. $A(\phi, T)$ is the decay and transmutation matrix, which is a function of the scalar flux ϕ and temperature T. The equations are written with a time dependence. For the direct equilibrium calculation in Griffin, the time derivative is simply set to zero and the resulting linear system solved with a direct method. Time integration accounting for these time derivatives which are present in the running-in simulation is discussed in the next section. As discussed previously, a key point to notice is that these equations are like two dimensional advection equations, on dimension being physical space the other burnup space.

$$\begin{aligned}\frac{d\vec{N}_{c,k,l,m}(t)}{dt} =& u_{k,m-1}\frac{a_{k,m-1}}{V_{k,m}}\vec{N}_{c,k,l,m-1}(t) + \frac{\bar{\rho}_{c,l-1,m}}{\Delta\tau_{l-1}}\vec{N}_{c,k,l-1,m}(t) \\ &- \left[\left(u_{k,m}\frac{a_{k,m}}{V_{k,m}} + \frac{\bar{\rho}_{c,l,m}}{\Delta\tau_l}\right) I + A(\phi(t), T(t))\right]\vec{N}_{c,k,l,m}(t)\end{aligned} \tag{1}$$

$$\begin{aligned}\frac{dn_{c,k,l,m}(t)}{dt} =& u_{k,m-1}\frac{a_{k,m-1}}{V_{k,m}}n_{c,k,l,m-1}(t) + \frac{\bar{\rho}_{c,l-1,m}}{\Delta\tau_{l-1}}n_{c,k,l-1,m}(t) \\ &- \left(u_{k,m}\frac{a_{k,m}}{V_{k,m}} + \frac{\bar{\rho}_{c,l,m}}{\Delta\tau_l}\right) n_{c,k,l,m}(t).\end{aligned} \tag{2}$$

2.1. Time Integration for Running-In

The discrete in time equations for Equation 1 and 2 are shown in Equations 3 and 4. Operator splitting is used to solve Equation 1 as shown in Equation 3, where Δt is the timestep, ℓ denotes the solution at the current time, $\ell + 1$ the solution at $t^\ell + \Delta t$, and $\ell*$ represents an intermediate step. Forward Euler is used to compute an intermediate solution $\vec{N}^{\ell*}_{c,k,l,m}$ from $\vec{N}^{\ell}_{c,k,l,m}$, accounting only for advection in space. The operator $\mathcal{S}_{\Delta t, A(\phi(t^\ell), T(t^\ell))}$ represents the Chebyshev rational approximation method (CRAM) [15], which is used to compute $\vec{N}^{\ell+1}_{c,k,l,m}$. Note the subscripts of the CRAM operator which denotes that the time dependence of the scalar flux and temperature is lagged by using the values from timestep ℓ. Also note the timestep used in $\mathcal{S}_{\Delta t, A(\phi(\ell))}$ is Δt. The time discretized version of Equation 2 is shown in Equation 4, this equation simply shows the application of forward Euler.

$$\begin{aligned} \vec{N}^{\ell*}_{c,k,l,m} &= \Delta t \begin{pmatrix} \frac{a_{k,m-1}}{V_{k,m}} u_{k,m-1} \vec{N}^{\ell}_{c,k,l,m-1} - \frac{a_{k,m}}{V_{k,m}} u_{k,m} \vec{N}^{\ell}_{c,k,l,m} + \\ \frac{\bar{\rho}_{c,l-1,m}}{\Delta \tau_{l-1}} \vec{N}^{\ell}_{c,k,l-1,m} - \frac{\bar{\rho}_{c,l,m}}{\Delta \tau_l} \vec{N}^{\ell}_{c,k,l,m} \end{pmatrix} + \vec{N}^{\ell}_{c,k,l,m} \\ \vec{N}^{\ell+1}_{c,k,l,m} &= \mathcal{S}_{\Delta t, A(\phi(t^\ell), T(t^\ell))} \vec{N}^{\ell*}_{c,k,l,m} \end{aligned} \tag{3}$$

$$n^{\ell+1}_{c,k,l,m} = \Delta t \begin{pmatrix} \frac{a_{k,m-1}}{V_{k,m}} u_{k,m-1} n^{\ell}_{c,k,l,m-1} - \frac{a_{k,m}}{V_{k,m}} u_{k,m} n^{\ell}_{c,k,l,m} + \\ \frac{\bar{\rho}_{c,l-1,m}}{\Delta \tau_{l-1}} n^{\ell}_{c,k,l-1,m} - \frac{\bar{\rho}_{c,l,m}}{\Delta \tau_l} n^{\ell}_{c,k,l,m} \end{pmatrix} + n^{\ell}_{c,k,l,m} \tag{4}$$

As documented in Ref. [11], the new running-in algorithms implemented in Griffin were verified by using the running-in code to compute an equilibrium core and comparing the results to the direct equilibrium core calculation already implemented in Griffin. Further verification such as convergence rates of the time integration will be documented in a future article.

2.2. Running-In Simulation Methodology

This section discusses various features of the model used to generate the sample multiphysics simulation results presented in Section 3. The running-in simulation is started from a critical core height calculation as described in Ref. [11] with the addition in this work that the initial temperatures are set from a Pronghorn calculation. The initial temperatures are shown in Figure 1b. The simulation is performed using multigroup diffusion with 9 energy groups.

Control rods are extended downward to an elevation of 7.2 m (see Figure 1a) at the start of the simulation. Since the model is in RZ-geometry, the number densities of control material is set so the rods are effectively modeled a "gray" curtain. The cusping treatment [16] included in Griffin is utilized. The control rod is withdrawn using a simple linear function. It is withdrawn starting at 50 days over the next 100 days to an elevation of 9.4 m. Control rods are included in the model to demonstrate the functionality, the specific movement regime of the rods is not optimized.

The power of the reactor is specified from the ratio of the volume of fuel pebbles at any time to the volume when the reactor is completely full of fuel pebbles. This ratio is multiplied by the nominal power level, thus the power is limited below the nominal value until all of the graphite pebbles have been removed. For the first 40 days, the ratio used for specifying the power is further multiplied by a quadratic function going from 0 to 1 to avoid the power being a relatively large non-zero value at time zero. The flow rate of coolant in the pronghorn model is held at a minimum of 6% the nominal value or is set by multiplying 1.2 times the nominal flow rate with the ratio of current power to nominal power. The flow rate is limited to the nominal value.

The target eigenvalue for the simulation is within a range of 1.003 to 1.007 and the method for staying within this target is currently to adjust the feed rate of pebbles. Using a combination of the feed rate and/or the control rods will be demonstrated in the future. The feed rate is controlled with simple proportional error logic using the error in the eigenvalue relative to a target of 1.005. This logic is wrapped in a bisection method which resets the timestep and picks a feed rate should the feed rate picked by the proportional controller fail to achieve an eigenvalue within the range at the end of a timestep.

3. MULTIPHYSICS RUNNING-IN SIMULATION DEMONSTRATION

Results from a sample running-in simulation are reviewed in this section. Table I describes how the pebbles are loaded with time based on the type of pebble which is discarded. Graphite pebbles are not reloaded, so when a graphite pebble leaves the bottom of the reactor, it is replaced with the ratio of pebbles described in Table I. For example, during the first 60 days graphite pebbles leaving the reactor are replaced with a fraction of 0.45 graphite pebbles and 0.55 of 5% fuel pebbles then after 80 days the fractions change to 0.3 and 0.7 respectively. Importantly, the makeup feed fractions apply only to discarded pebbles. The burnup limit assumed in this simulation is 60420 MWd/tU for 5% enriched fuel pebbles and is 135946 MWd/tU for the 15.5% enriched fuel pebbles. Early in the simulation, when a 5% enriched fuel pebble leaves the bottom of the reactor, it may be below the burnup limit in which case it is reloaded to the top of the core. If it is beyond the burnup limit, the makeup feed is determined by Table I, for example if the time is greater than 60 days and less than 80 days, the 5% enriched fuel pebbles discarded are replaced with a fraction of 0.2 graphite pebbles and 0.8 fresh 5% enriched fuel pebbles. Figure 2 shows the total volume of the three pebble types in the reactor during the running-in simulation.

Figure 3 shows the maximum power density throughout the running-in simulation. The maximum power spikes to an unacceptably high level around 130 days. The feed regime of pebbles in Table I can be further optimized from the sample values used in this calculation to avoid this power spike. Control rod movement could also be adjusted as the control rod is being withdrawn during this time the spike in power density occurs. The effect of the control rod on power generation can be seen in Figure 4. The pebble feed rate, k-eigenvalue, total reactor power, and average discharge burnup are all plotted for the duration of the running-in simulation in Figure 5. Note the oscillations in the k-eigenvalue and pebble feed rate plot. This is caused by the settings of the proportional controller responsible for picking a feed rate (discussed further in Section 2.2). These oscillations can be removed with further optimization of the controller in the future.

A benefit of the modelling approach used in Griffin is that the burnup of pebbles is computed directly. The average core burnup is plotted in Figure 6 where some interesting features can be seen. Notice that from 218 to 375 days, a collection of burned pebbles moves down the core, but then at 406 days the average burnup at the top of the core decreases. The reason for this is that the area of higher burnup in the plot is due to the 5 % enriched fuel pebbles. They have a lower burnup limit and as they are leaving the core around 375 days, they are discarded and fresh 20 % enriched fuel pebbles makeup the difference in the fresh feed. These pebbles have no burnup and thus the average burnup drops near the top of the core. This is likely not desirable and could optimized in future calculations, but this results shows what can be visualized from a Griffin simulation since the burnup is explicitly calculated.

Forward Euler (described in Section 2.1) is only conditionally stable. A relatively small fixed timestep of 15 hours was used in this work although a larger timestep of several days could be used without violating stability conditions. Each timestep including the Pronghorn calculation takes only approximately 10 seconds using a single processor. Implementation of an implicit time integration method may be useful in the future, however, this work shows that the simple explicit method should be useful in many cases for realistic simulations going forward.

Table I. Pebble makeup feed specifications as a function of the discarded pebble types.

Discarded Pebble Type	Fraction of Pebble Type in Makeup Feed		
	Graphite Only	5 % Enriched Fuel	15.5 % Enriched Fuel
Time <60 days			
Graphite Only	0.45	0.55	0.0
5 % Enriched Fuel	0.5	0.5	0.0
15.5 % Enriched Fuel	0.0	0.0	1.0
Time <80 days			
Graphite Only	0.3	0.7	0.0
5 % Enriched Fuel	0.2	0.8	0.0
15.5 % Enriched Fuel	0.0	0.0	1.0
Time <105 days			
Graphite Only	0.1	0.9	0.0
5 % Enriched Fuel	0.0	1.0	0.0
15.5 % Enriched Fuel	0.0	0.0	1.0
Time <125 days			
Graphite Only	0.0	1.0	0.0
5 % Enriched Fuel	0.0	1.0	0.0
15.5 % Enriched Fuel	0.0	0.0	1.0
Time <320 days			
Graphite Only	0.0	0.0	1.0
5 % Enriched Fuel	0.0	0.7	0.3
15.5 % Enriched Fuel	0.0	0.0	1.0
Time <420 days			
Graphite Only	0.0	0.0	1.0
5 % Enriched Fuel	0.0	0.5	0.5
15.5 % Enriched Fuel	0.0	0.0	1.0
Time ≥ 420 days			
Graphite Only	0.0	0.0	1.0
5 % Enriched Fuel	0.0	0.0	1.0
15.5 % Enriched Fuel	0.0	0.0	1.0

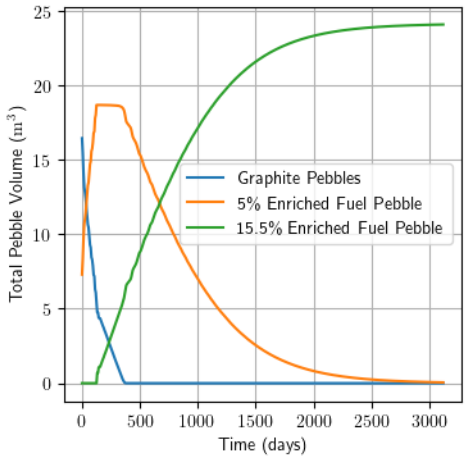

Figure 2. Total volume of each pebble type shown through time.

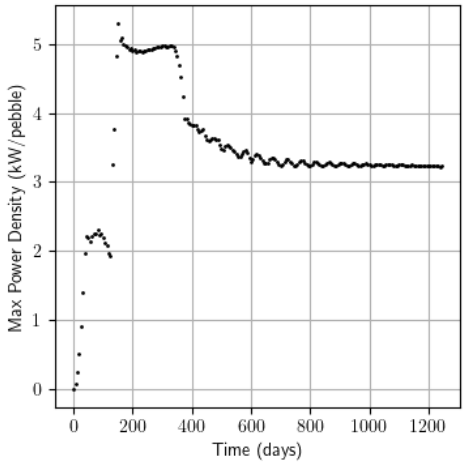

Figure 3. Maximum pebble power density plotted through time.

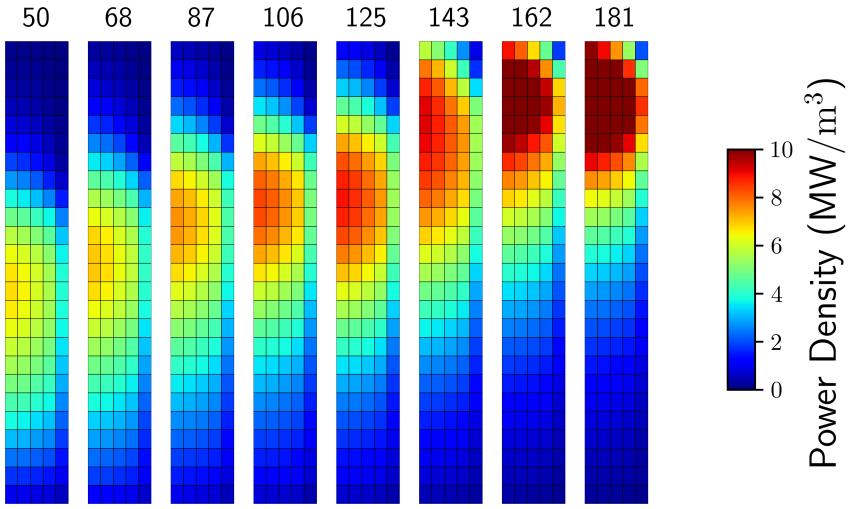

Figure 4. Power density for eight select times during the initial part of the running-in simulations. The numbers on top of the plots are the time in days.

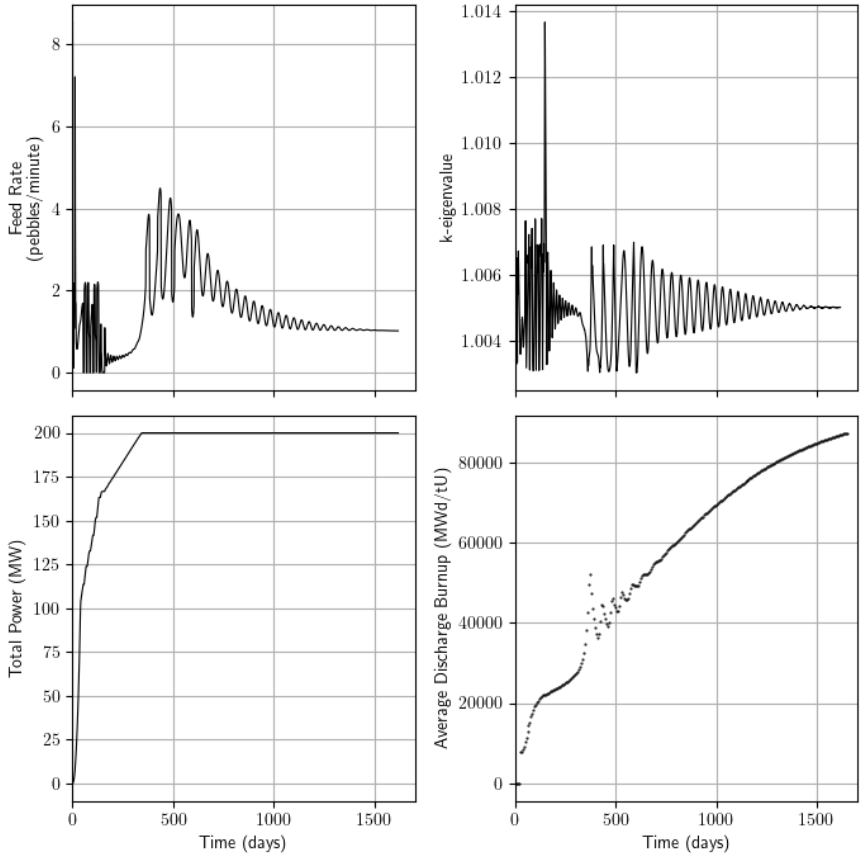

Figure 5. The pebble feed rate, k-eigenvalue, total reactor power, and average discharge burnup all plotted for the duration of the running-in simulation.

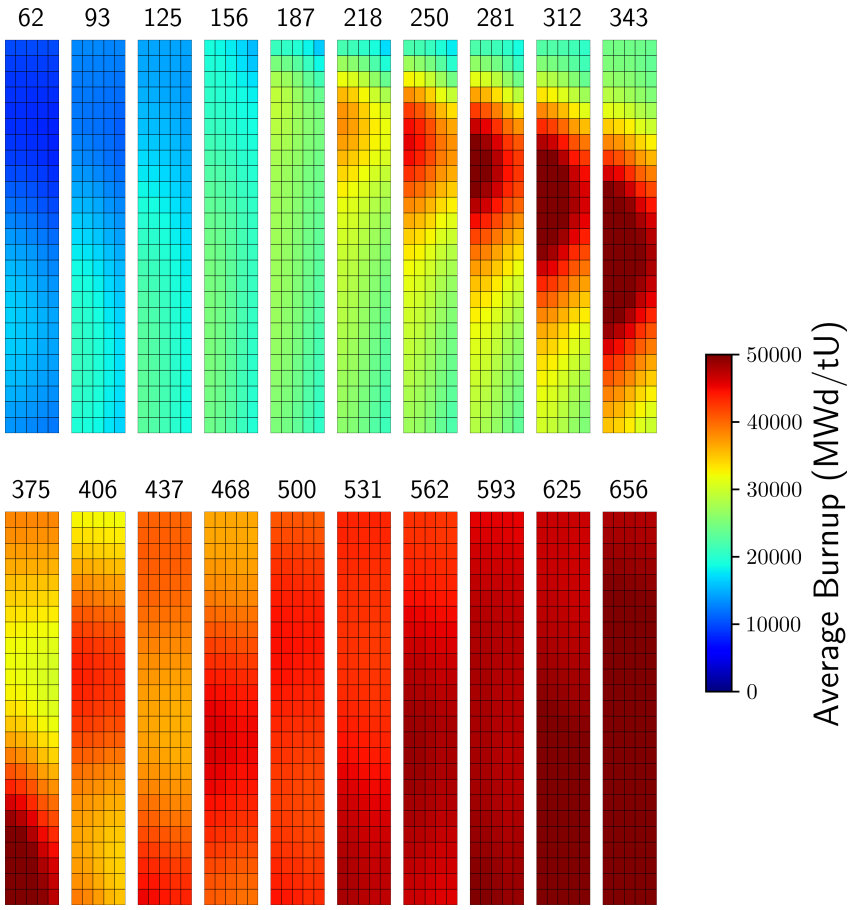

Figure 6. Average burnup for 24 select times during the initial part of the running-in simulation. The numbers on top of the plots are the time in days.

4. CONCLUSIONS

Because Griffin is a MOOSE based application, it is easily coupled to other MOOSE based applications for multiphysics simulations. While significant code changes were made to implement a running-in simulation capability in Griffin, the interfaces to other applications remain essentially unchanged. The Pronghorn input used for the sample running-in simulation is nearly the same as one used for an equilibrium core calculation. Results from more sophisticated numerical methods will be published in the future and compared with the first order operator splitting and forward Euler time integration used in this work. However, the results in this work indicate that even these simple numerical methods are useful.

The RZ-geometry model used in this work as well as higher fidelity models with finer detail included, though still in RZ-geometry, take minimal computational resources. For this reason, these models will be useful for optimization studies of the running-in phase where many thousands of simulations can be performed. The running-in results presented in this work have not been optimized, they are meant to demonstrate some features of the new capability. Results published in the future will make use of parameter studies to optimize important procedures such as the pebble feed composition throughout time and the movement of the control rods.

ACKNOWLEDGEMENTS

This work was supported by the U.S. Department of Energy (DOE), Office of Nuclear Energy, under contract DE-AC07-05ID14517 for DOE Idaho Operations Office and supported by the DOE Nuclear Energy Advanced Modeling and Simulation Program.

REFERENCES

[1] A. D. Lindsay, D. R. Gaston, C. J. Permann, J. M. Miller, D. Andrš, A. E. Slaughter, F. Kong, J. Hansel, R. W. Carlsen, C. Icenhour, L. Harbour, G. L. Giudicelli, R. H. Stogner, P. German, J. Badger, S. Biswas, L. Chapuis, C. Green, J. Hales, T. Hu, W. Jiang, Y. S. Jung, C. Matthews, Y. Miao, A. Novak, J. W. Peterson, Z. M. Prince, A. Rovinelli, S. Schunert, D. Schwen, B. W. Spencer, S. Veeraraghavan, A. Recuero, D. Yushu, Y. Wang, A. Wilkins, and C. Wong. "2.0 - MOOSE: Enabling massively parallel multiphysics simulation." *SoftwareX*, **volume 20**, p. 101202 (2022). URL https://www.sciencedirect.com/science/article/pii/S2352711022001200.

[2] R. Stewart, P. Balestra, D. Reger, and E. Merzari. "Generation of localized reactor point kinetics parameters using coupled neutronic and thermal fluid models for pebble-bed reactor transient analysis." *Annals of Nuclear Energy*, **volume 174**, p. 109143 (2022). URL https://www.sciencedirect.com/science/article/pii/S0306454922001785.

[3] G. L. Giudicelli, A. Abou-Jaoude, A. J. Novak, A. Abdelhameed, P. Balestra, L. Charlot, J. Fang, B. Feng, T. Folk, R. Freile, T. Freyman, D. Gaston, L. Harbour, T. Hua, W. Jiang, N. Martin, Y. Miao, J. Miller, I. Naupa, D. O'Grady, D. Reger, E. Shemon, N. Stauff, M. Tano, S. Terlizzi, S. Walker, and C. Permann. "The Virtual Test Bed (VTB) Repository: A Library of Reference Reactor Models Using NEAMS Tools." *Nuclear Science and Engineering*, **volume 197**(8), pp. 2217–2233 (2023). URL https://doi.org/10.1080/00295639.2022.2142440.

[4] Z. M. Prince, C. Brennan, M. Turkmen, P. Balestra, and G. Strydom. "Reduced Order Models Generation for HTGRs Pebble Shuffling Procedure Optimization Studies." Technical Report INL/RPT-22-68865, Idaho National Laboratory (2022). URL https://www.osti.gov/biblio/1901800.

[5] Balestra, Paolo, Schunert, Sebastian, Carlsen, Robert W, Novak, April J, DeHart, Mark D, and Martineau, Richard C. "PBMR-400 BENCHMARK SOLUTION OF EXERCISE 1 AND 2 USING THE MOOSE BASED APPLICATIONS: MAMMOTH, PRONGHORN." *EPJ Web Conf*, **volume 247**, p. 06020 (2021). URL https://doi.org/10.1051/epjconf/202124706020.

[6] S. Schunert, J. Ortensi, Y. Wang, P. Balestra, M. Jaradat, O. Calvin, J. Hanophy, and L. Harbour. "An equilibrium core depletion algorithm for pebble-bed reactors in the Griffin code." *Annals of Nuclear Energy*, **volume 192**, p. 109980 (2023). URL https://www.sciencedirect.com/science/article/pii/S0306454923002992.

[7] J. Ortensi, C. M. Mueller, S. Terlizzi, G. Giudicelli, , and S. Schunert. "Fluoride-Cooled High-Temperature Pebble-Bed Reactor Reference Plant Model." Technical Report INL/RPT-23-72727, Idaho National Laboratory (2023).

[8] J. Zhang, F. Li, and Y. Sun. "Physical Analysis of the Initial Core and Running-In Phase for Pebble-Bed Reactor HTR-PM." *Science and Technology of Nuclear Installations*, **volume 2017** (2017). URL https://doi.org/10.1155/2017/8918424.

[9] E. Teuchert, U. Hansen, and K. A. Haas. "VSOP - computer code system for reactor physics and fuel cycle simulation." Technical Report JUEL–1649, Kernforschungsanlage Juelich G.m.b.H. (Germany, F.R.). Inst. fuer Reaktorentwicklung (1980).

[10] R. Stewart, P. Balestra, D. Reger, E. Merzari, and G. Strydom. "High-fidelity simulations of the run-in process for a pebble-bed reactor." *Annals of Nuclear Energy*, **volume 195**, p. 110193 (2024). URL https://www.sciencedirect.com/science/article/pii/S0306454923005121.

[11] J. Hanophy, H. Park, V. Labouré, Y. Jung, S. Schunert, Y. Wang, and J. Ortensi. "Initial Demonstration of New Griffin Technologies for Simulating the Running-In Phase of Pebble-Bed Reactors." Technical Report INL/RPT-23-74913, Idaho National Laboratory (2023).

[12] A. J. Novak, R. W. Carlsen, S. Schunert, P. Balestra, D. Reger, R. N. Slaybaugh, and R. C. Martineau. "Pronghorn: A Multidimensional Coarse-Mesh Application for Advanced Reactor Thermal Hydraulics." *Nuclear Technology*, **volume 207**(7), pp. 1015–1046 (2021). URL https://doi.org/10.1080/00295450.2020.1825307.

[13] R. Stewart, P. Balestra, D. Reger, and G. Strydom. "Novel Pebble Shuffling Capabilities to Generate Reduced Order Models Training Databases." Technical Report INL/RPT-22-68918, Idaho National Laboratory (2022).

[14] S. Schunert, J. R. Brennan, M. K. Jaradat, and P. Balestra. "Assessment of the New NEAMS Tools FVM Capabilities for the Simulation of HTGRs." Technical Report INL/RPT-23-74236, Idaho National Laboratory (2023).

[15] M. Pusa and J. Leppänen. "Computing the Matrix Exponential in Burnup Calculations." *Nuclear Science and Engineering*, **volume 164**(2), pp. 140–150 (2010). URL https://doi.org/10.13182/NSE09-14.

[16] S. Schunert, Y. Wang, J. Ortensi, V. M. Labouré, F. N. Gleicher, M. D. DeHart, and R. C. Martineau. "Control Rod Treatment for FEM Based Radiation Transport Methods." *Annals of Nuclear Energy*, **volume 127**, pp. 293–302 (2019).